

Numerical simulation of the Gailitis dynamo

David Moss¹
School of Mathematics
University of Manchester
Oxford Rd
Manchester M13 9PL
UK

Abstract

The linear magnetohydrodynamic equations are solved with vacuum surface boundary conditions in a thick spherical shell, where the only fluid motions are meridional ‘rolls’. These motions are similar to those studied by Gailitis (1970), except that in that paper the motions were confined to toroidal annuli, with minor and major axes a and c respectively, and $a/c \ll 1$. The seminal result of Gailitis, that such motions excite magnetic fields with axis of symmetry perpendicular to the axis of symmetry of the velocity field, is illustrated for cases where Gailitis’s conditions are relaxed. In particular, the parity properties of the dynamo-generated fields depend on the sense of the fluid motions in the same manner as found by Gailitis. An attempt is made to compare predicted and computed marginal dynamo numbers – a plausible agreement is obtained. Finally, when the parity of the fluid motion is reversed, a new class of nonaxisymmetric oscillatory dynamo solutions is obtained.

Keywords: magnetic fields – MHD – Gailitis dynamo – dynamo theory

1 Introduction

Gailitis (1970 – see also Moffatt 1978) produced one of the first accepted proofs of the existence of (kinematic) fluid dynamo action, others being by Herzenberg (1958) and Backus (1958). Ponomarenko (1973) shortly afterwards produced another example. In Gailitis’s model, two azimuthal ‘rolls’ of fluid, distributed in rings about a common axis, produce a large-scale magnetic field with axis of symmetry perpendicular to this axis - ‘perpendicular-dipole’ or ‘perpendicular-quadrupole’ like fields. Given the seminal importance of this proof, and the current astrophysical dynamo ‘industry’, it is perhaps rather surprising that this analytical result has not been extensively reproduced (or supported) by numerical simulation. In fact, recently anecdotal reports have been circulating of failure to reproduce dynamo action by numerical simulation in a Gailitis-like situation, but it seems that the fluid may there have effectively extended to infinity. These reports appear to be inconsistent with the work of Moss (1990), who in the context of Cp star magnetism obtained a positive growth rate from an imposed ‘Eddington-Sweet’-like meridional circulation that extended throughout a thick spherical shell.

In contrast, the early analytical proof of dynamo action by Herzenberg (1958) was recently illustrated numerically for the first time by Brandenburg, Moss and

¹e-mail: moss@ma.man.ac.uk

Soward (1998), who additionally found a new class of oscillating solutions.

In this paper we report on numerical experiments in a geometry similar to that studied by Gailitis, and dynamo action is shown conclusively to occur. For a range of parameters the salient results of the analysis by Gailitis (1970) are reproduced – specifically that meridional rolls with downward motion on the sides nearer to the equatorial plane in each hemisphere produce even parity (‘perpendicular-dipole’-like) fields, whereas motion in the opposite sense preferentially excites fields of the opposite parity. Such magnetic fields, proportional to $e^{i\mu\phi}$ with $\mu = 1$ and ϕ the azimuthal angle, are commonly referred to as being of S1 and A1 type respectively (e.g. Krause and Rädler 1980). These velocity fields have even parity with respect to the equatorial plane. A novel feature is that for an imposed circulation with odd parity with respect to the equatorial plane, a dynamo with *oscillatory* energy and parity is found to be excited.

2 The model

In Gailitis’s original model, the fluid motions are confined to two coaxial toroidal annuli, of minor radii a , situated at distance d from the equatorial plane and distance c from the axis (Figure 1), with $a/c, a/d \ll 1$. He found that dynamo action occurred for Reynolds numbers $Rm = Va/\eta > (c/a)^2 T_m(d/c)$, where V is a typical fluid velocity, η is the uniform magnetic diffusivity and T_m is a known function.

We used a strictly linear version of the general nonlinear nonaxisymmetric dynamo code described in Moss, Tuominen and Brandenburg (1991), removing all need for transformation of nonlinear terms between real and Fourier space. No conventional dynamo drivers (α -effect, differential rotation) were included, and the only fluid motions were axisymmetric and in meridian planes (azimuthal wave number $m = 0$). Thus it was possible to integrate in isolation the $m = 1$ components of the non-dimensional MHD equation

$$\frac{\partial \mathbf{B}}{\partial \tau} = \nabla \times (\mathbf{v} \times \mathbf{B} - \nabla \times \mathbf{B}). \quad (1)$$

This equation has been nondimensionalized with respect to unit of length the radius R of the computational volume, the uniform diffusivity η_0 , and time unit R^2/η_0 . (Thus the diffusivity does not appear explicitly in equation (1).) The magnetic field is expressed in terms of ‘superpotentials’ Φ and Ψ for the poloidal and toroidal parts of the field, $\mathbf{B} = \mathbf{B}_P + \mathbf{B}_T = \nabla \times (\Phi \hat{\mathbf{r}}) + \nabla \times \nabla \times (\Psi \hat{\mathbf{r}})$ (e.g. Chandrasekhar 1961). The code was implemented on a spatial grid in the meridian (r, θ) plane, with a computational grid distributed uniformly over M radial and N latitudinal points covering a spherical shell $r_0 \leq r \leq 1$, $0 \leq \theta \leq \pi$ respectively, where (r, θ, ϕ) are spherical polar coordinates, and r is the fractional radius in the computational volume. Standard values were $M = 61$, $N = 101$, $r_0 = 0.2$. The initial state was usually an arbitrary small ‘seed’ field, except that some of the higher resolution computations were continued from a lower resolution solution.

The meridional velocity is given in dimensionless form by a streamfunction ψ , where

$$\mathbf{v} = \left(\frac{1}{r^2 \sin \theta} \frac{\partial \psi}{\partial \theta}, -\frac{1}{r \sin \theta} \frac{\partial \psi}{\partial r} \right), \quad (2)$$

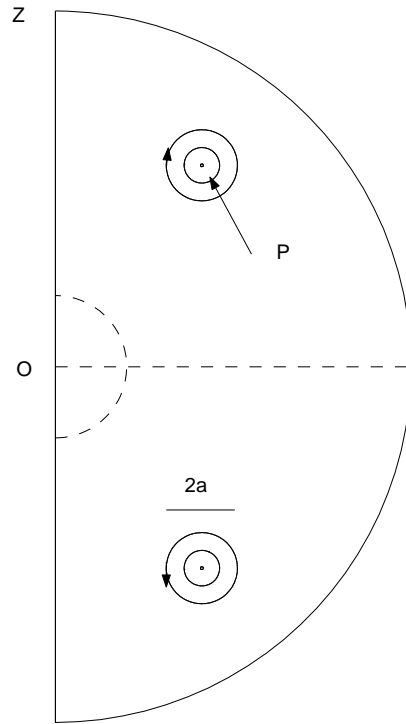


Figure 1: A cross-section in a meridian plane showing the configuration of the Gailitis model. In the text, a is the minor radius of the annuli centred on P and its reflection in the equator, c is the major radius, ie the distance of P from the axis OZ , and d is the distance of P from the equatorial plane. For the flows considered in this paper, the arrows indicate the direction of the fluid motion for positive factors A in equation (3).

with

$$\psi = A(r - r_0)^2(1 - r)^2 \sin^m \theta \cos^n \theta \quad (3)$$

– the density has been taken as uniform, and so does not formally appear. m and n are positive integers and A is an adjustable constant, that controls the magnetic Reynolds number of the flow for given m and n . Thus when n is odd and $A > 0$, motions are downwards near the equatorial plane and upwards nearer the poles, and *vice versa*. Higher values of m, n give more localized velocity distributions. To some extent the value of m controls the angular distance of the rolls from the axes $\theta = 0, \pi$, and n controls the angular distance from the equatorial plane $\theta = \pi/2$.

At $r = 1$ the field was fitted to an external vacuum field, and the standard lower boundary conditions were that $\Phi = \Psi = 0$ on $r = r_0$, implying that $\mathbf{B}_T = \mathbf{0}$, $\hat{\mathbf{r}} \cdot \mathbf{B}_P = 0$ there. We also investigated an ‘overshoot’ boundary condition at $r = r_0$,

$$\frac{\partial(\Phi, \Psi)}{\partial r} = \frac{(\Phi, \Psi)}{\delta}, \quad (4)$$

which might be considered as roughly simulating decay of the field over a distance of order δ below the boundary. This was found not to change significantly the results; taking $\delta = 0.05$ increased the marginal magnetic Reynolds number by about 10% in a typical case, and $\delta = 0.2$ gave a larger increase. The most noticeable effect on the field structure was a modest reduction in radial gradients near $r = r_0$.

Gross symmetry properties of both magnetic and velocity fields are described by a parity parameter P , where $P = +1/-1$ for fields with radial components that are respectively of even/odd symmetry with respect to the equator (e.g. Moss et al. 1991).

It is useful to define the parity of magnetic and velocity fields by

$$P = \frac{E^+ - E^-}{E^+ + E^-}, \quad (5)$$

where E^+, E^- are the energies in the part of the relevant field that are respectively symmetric, antisymmetric with respect to the rotational equator (see, e.g., Moss et al. 1991).

Equation (1) is linear, and was integrated until an eigenmode was reached, showing an exponential growth of the global magnetic energy with time, with unchanging spatial structure.

3 Results

3.1 Flows with $m = 6, n = 3$

We first describe results taking $m = 6, n = 3$, giving streamlines as shown in Figure 2a. With a seed field that is of mixed (intermediate) parity with respect to the equatorial plane $\theta = \pi/2$ and $A > 0$, for large enough values of A steadily growing magnetic fields of even parity are found. The marginal value is $A_c \approx 2.4 \times 10^4$. The distribution of the radial component of field with radius at $\theta = 60^\circ, \phi = 0$ is shown in Figure 3a, and the surface distribution of radial field is shown in Figure 4a.

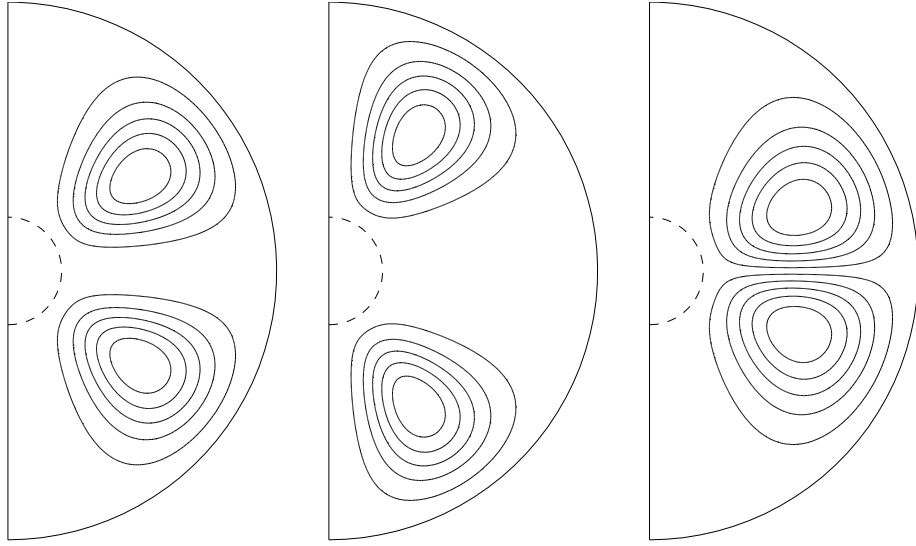


Figure 2: The streamlines of the meridional flows for a) $m = 6, n = 3$; b) $m = 3, n = 7$; c) $m = 6, n = 1$. Radial velocities are positive near the poles. The broken semicircle indicates the lower boundary of the computational domain at $r = r_0 = 0.2$.

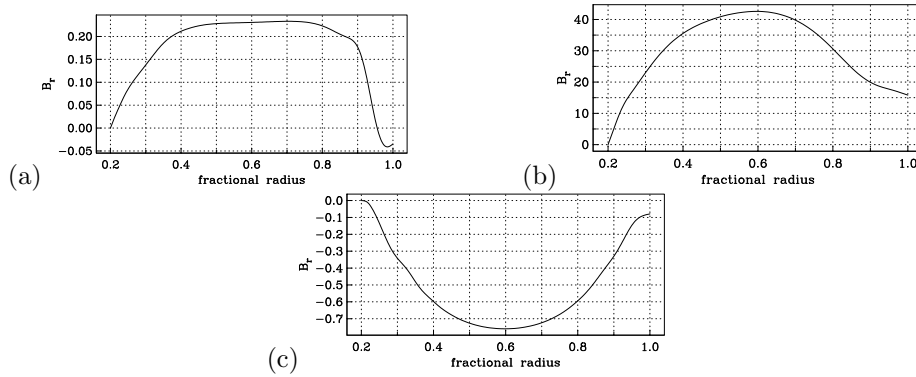


Figure 3: Dependence of radial field on radius at $\theta = 60^\circ$ for a) $m = 6, n = 3, A = 10^5$; b) $m = 3, n = 7, A = 10^5$; c) $m = 6, n = 1, A = 9 \times 10^4$. The vertical scales are arbitrary in magnitude and sign.

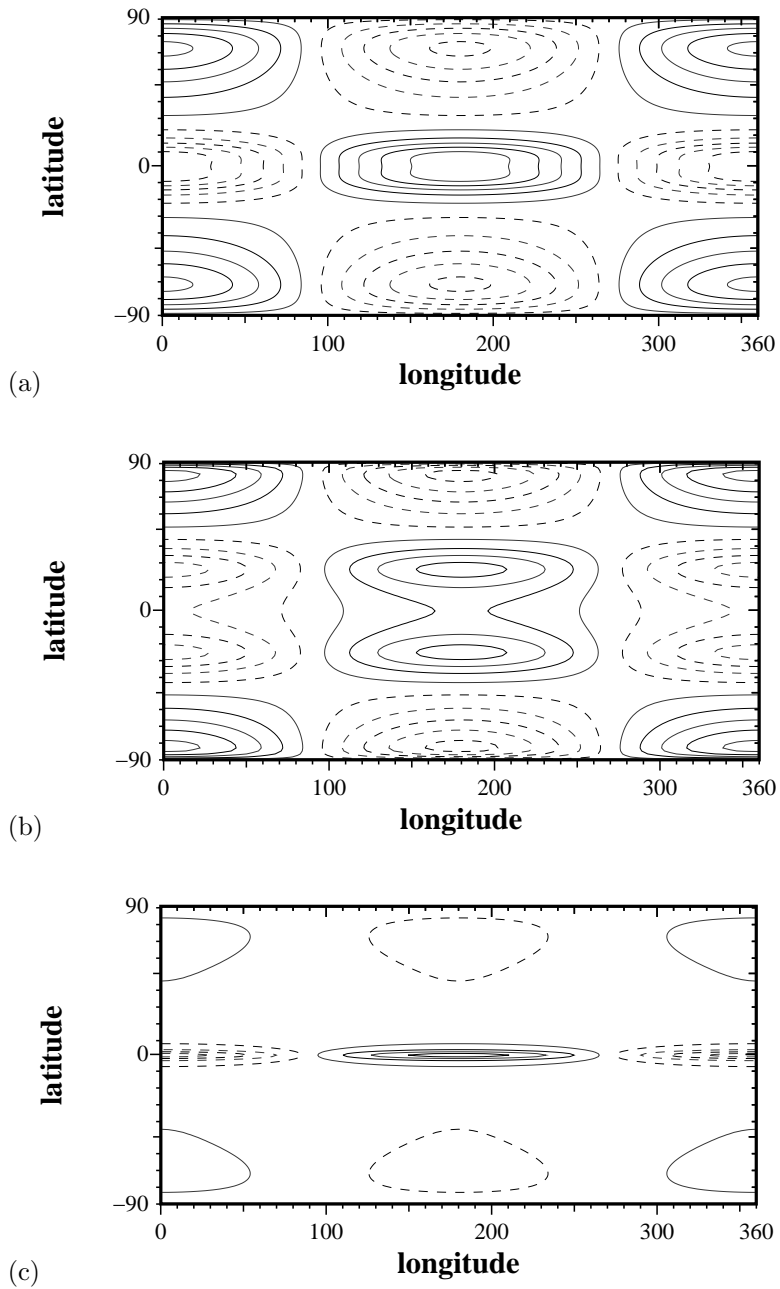


Figure 4: Equally spaced contours of surface radial field for a) $m = 6, n = 3, A = 10^5$; b) $m = 3, n = 7, A = 10^5$; c) $m = 6, n = 1, A = 9 \times 10^4$. Solid and broken contours indicate positive and negative values respectively.

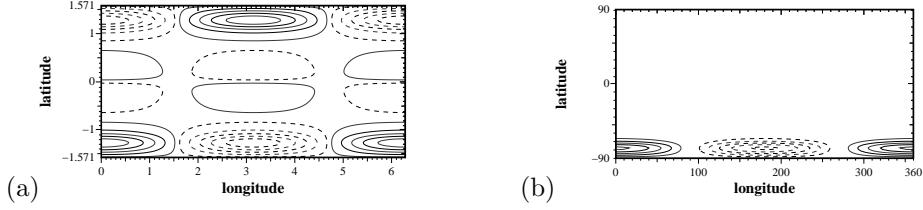


Figure 5: Equally spaced contours of surface radial field: (a) $m = 6, n = 3, A = 6 \times 10^4$, flow reversed, (b) $m = n = 6, A = 5 \times 10^5$, odd parity velocities. Solid and broken contours indicate positive and negative values respectively.

Table 1: The dependence of growth rate Γ on resolution when $m = 6, n = 3, A = 10^5$.

M	N	Γ
61	101	8.7
101	201	8.6
201	201	8.8

In order to check the dependence of these results on numerical resolution, for the case $A = 10^5$ we found the results for the growth rate of the eigenmode, $\Gamma = d \log |\mathbf{B}| / dt$, that are shown in Table 1. From this we deduce that the standard spatial resolution $M = 61, N = 101$ is adequate for our purposes.

When $A < 0$ the flow is reversed, i.e. the radial velocity is negative near the poles. For large enough $|A|$ exponentially growing fields with odd parity are found. The marginal value then is $A_c \approx -3.9 \times 10^4$. Contours of surface radial field are shown in Figure 5.

3.2 A flow localized at higher latitudes: $m = 3, n = 7$

When $m = 3, n = 7$ the streamlines are as shown in Figure 2b. Following the same procedure as described in section 3.1, the parity of the fields evolved according to the sign of A as for $m = 6, n = 3$. The marginal value of A for fields of even parity is $A_c \approx 1.6 \times 10^4$. The spatial structure of the eigensolutions appears quite similar to that for the case $m = 6, n = 3$ – see Figures 3b, 4b.

3.3 A flow localized near the equator: $m = 6, n = 1$

Streamlines are shown in Figure 2c – this flow is much more concentrated to the equatorial plane than those discussed above in sections 3.1, 3.2, and so are the resulting dynamo-excited fields. The standard resolution $M = 61, N = 101$ did not produce satisfactory solutions. However with $M = N = 201$ the behaviour of the solutions did appear satisfactory. It was impractical to increase the resolution further, and so the dependence on spatial resolution could not be checked in this case. Thus the results in this section must be regarded as estimates. The marginal value is significantly larger than for the cases described in sections 3.1 and 3.2, with $A_c \approx 8.1 \times 10^4$. The dependence of radial field

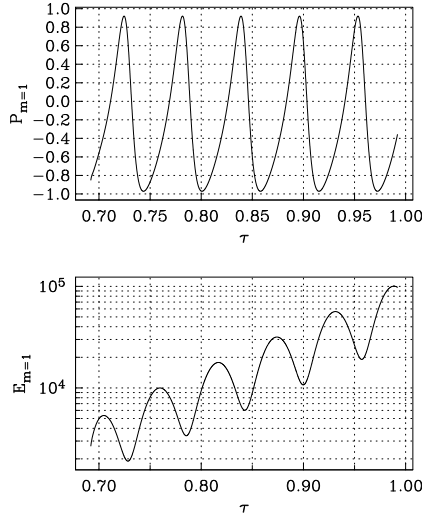


Figure 6: The variation of magnetic energy (top panel) and parity (lower panel) with time τ : odd parity velocities, $m = n = 6$, $A = 5 \times 10^4$.

on radius and surface radial field contours are shown in Figures 3c and 4c respectively.

3.4 Flows with odd parity

The flows investigated above all have even parity with respect to the equator, as had the flow investigated by Gailitis (1970). We also investigated a flow with the opposite (odd) parity – obtained by either taking n even (equation (3)), or by explicitly reversing the flow in the southern hemisphere when n is odd. (Equivalently, for n odd, opposite signs of A can be taken in the different hemispheres.) cursory inspection of the parity properties of equation (1) shows that pure parity solutions are no longer possible. Nevertheless, a dynamo again is excited for large enough A . The solutions display oscillatory behaviour of both magnetic energy and field parity, the latter varying between extremes close to $P = \pm 1$. The case $m = n = 6$ is typical. Then $A_c \approx 4 \times 10^5$ – much larger than found in similar cases with even parity velocities, and the variation of magnetic energy and parity with time for a slightly supercritical case is shown in Figure 6. A snapshot of surface radial field contours when $P \approx -0.35$ is given in Figure 5b.

4 Discussion

The gross outcomes of the numerical experiments with n odd (sections 3.1, 3.2, 3.3) agree well with the analytical results of Gailitis (1970), (necessarily) removing the restriction to $a/c, a/d \ll 1$, for the case of motions confined to a spherical volume with exterior vacuum. Previously, analysis has only provided the marginal values of the parameter A , and so it is of interest to attempt to compare the marginal magnetic Reynolds numbers with Gailitis’s predictions.

Table 2: Estimates for the marginal magnetic number, calculated as discussed in section 4, for the cases $m, n = (3, 7), (6, 3)$ and $(6, 1)$.

m, n	A_c	a_{eff}	c	d	u_{max}	u_{rms}	u_{rms1}	Rm_{c1}	Rm_{c2}	Rm_{c3}	$Rm_c(G)$
3, 7	16000	0.12	0.33	0.50	750	230	550	90	28	66	24
6, 3	24000	0.12	0.49	0.35	570	220	410	68	26	49	36
6, 1	81000	0.12	0.55	0.23	7290	2830	5330	800	310	590	60

Defining $Rm = Va/\eta_0$, where V is a mean velocity in the annuli, Gailitis found a marginal magnetic Reynolds number $Rm_c = (c/a)^2 T_m(d/c)$, where c is the major radius of the torus and T_m is a function of order unity for the range of parameters that might be appropriate for our numerical experiments. Of course, the analysis giving this estimate for Rm_c neglects terms of order a/c and a/d , and in our models these are of order unity.

Given the more distributed, quite non-uniform, flows considered above, it is hard to make an exact comparison. However if d is taken as the distance of the centres of the circulation cells from the equator, c the distance from the axis, and a_{eff} is a measure of the half width of the cells, then using a suitable value for the velocity a prediction for Rm_c can be obtained, say $Rm_c(G)$. From the results described above we can define a corresponding numerical estimate of $Rm_c(N) = a_{eff} V_{eff}$, where V_{eff} is a typical (dimensionless) velocity given by equations (2) and (3). The appropriate choice for V_{eff} is unclear, but *a priori* plausible choices might be either the maximum value of the circulation speed, giving say Rm_c , or u_{rms} , the r.m.s. value over the whole domain (Rm_{c2}), or perhaps even u_{rms1} , the r.m.s. value over the region where $u > \frac{1}{2}u_{max}$, yielding Rm_{c3} .

In Table 2 the relevant parameters and estimates are given for three models. For $m, n = (6, 3)$ and $(6, 7)$, approximate agreement is found between marginal Reynolds numbers as given by naive application of Gailitis's expression, and estimated above by $Rm_{ci}, i = 2$ or 3 . However, the agreement is significantly worse when $m = 6, n = 1$, i.e. when the vortices are located close to the equator. It may be relevant in this context that this is the case where a/d takes its largest value. Given that Gailitis's analysis does not claim to be valid for the parameter range studied here, the most that can be claimed is that these figures are not obviously grossly inconsistent.

5 Conclusions

A straightforward numerical simulation without any numerical truncations has reproduced the main thrust of the results of Gailitis (1970), relaxing his conditions $a/c, a/d \ll 1$. The predicted relation between flow and field geometries is reproduced, and the marginal magnetic Reynolds numbers can be estimated to be of the same order as predicted by a naive application of Gailitis's result. Note that in the limit considered by Gailitis, the marginal values increase approximately as $(c/a)^2$, and so become large. However, for the parameters considered above the critical magnetic Reynolds numbers are of comparable magnitude to

those of the Ponomarenko (1973) dynamo. The calculations are exact in the context of the grid point method (Dufort-Frankel) used for the integration in the r, θ plane. For the first time, the geometry of the eigenmodes has been determined. This part of the investigation, reported in section 3.1, is also broadly consistent with the results of Moss (1990) where the flow field was a modified Eddington-Sweet circulation, although in the computations described here the velocity field is rather more localized. Note that Moss (1990) uses an independent, and quite different, numerical code.

For circulations that have odd parity with respect to the equator (i.e. the opposite to the case considered by Gailitis) oscillatory dynamo modes are excited. Gailitis's analysis did not address this case, and thus these are previously unknown dynamo solutions. Interestingly, Brandenburg et al. (1998) also discovered a previously unsuspected class of oscillatory solutions in their numerical investigation of the Herzenberg dynamo.

Acknowledgements

Thanks are due to Leon Mestel and Dmitri Sokoloff for comments on a draft version of this paper. The final version was also improved by the reports from anonymous referees.

References

- Backus, G., A class of self-sustaining dissipative spherical dynamos, *Ann. Phys.*, **4**, 372-447 (1958)
- Brandenburg A., Moss D. and Soward A., New results for the Herzenberg dynamo: steady and oscillatory solutions, *Proc. R. Soc. A*, **454**, 1283-1300 (1998)
- Chandrasekhar, S., *Hydrodynamic and Hydromagnetic Stability*, Clarendon Press, Oxford (1961)
- Gailitis, A., Self-excitation of a magnetic field by a pair of annular vortices, *Mag. Gidrod.*, **6**, 19-22 (1970) (English translation: *Magnetohydrodynamics*, **6**, 14-17 (1970))
- Krause, F. and Rädler, K.-H., *Mean-Field Magnetohydrodynamics and Dynamo Theory*, Pergamon Press, Oxford, 1980
- Herzenberg, A., Geomagnetic dynamos, *Phil. Trans. R. Soc. A*, **250**, 543-583 (1958)
- Moffatt, H.K., *Magnetic field generation in electrically conducting fluids*, CUP, Cambridge (1978)
- Moss, D., A Gailitis-type dynamo in the magnetic CP stars?, *Mon. Not. R. astr. Soc.*, **243**, 537-542 (1990)
- Moss, D., Tuominen, I. and Brandenburg, A., Nonlinear nonaxisymmetric dynamo models for cool stars, *Astron. Astrophys.*, **245**, 129-135 (1991)
- Ponomarenko, Yu. B., Theory of the hydromagnetic generator, *Zh. Prikl. Melch. Telch. Fiz. (USSR)*, **6**, 47-51 (1973) (English translation: *J. Appl. Mech. Techn. Phys.* **14**, 775-778 (1973))